Journal of Petroleum Science and Engineering 172 (2019) 1025–1033

Contents lists available at ScienceDirect

Journal of Petroleum Science and Engineering

journal homepage: www.elsevier.com/locate/petrol

Determination of pore compressibility and geological reserves using a new form of the flowing material balance method

Guofeng Han[a], Yuewu Liu[a,*], Liang Sun[b], Min Liu[c], Dapeng Gao[a], Qi Li[d]

[a] Institute of Mechanics, Chinese Academy of Sciences, Beijing, 100190, China
[b] PetroChina Research Institute of Petroleum Exploration & Development, Beijing, 100083, China
[c] Exploration and Development Research Institute of PetroChina Tarim Oilfield Company, Korla, Xinjiang, 841000, China
[d] North China University of Technology, Beijing, 100144, China

ARTICLE INFO

Keywords:
Flowing material balance method
Pore compressibility
Geological reserve
Material balance equation

ABSTRACT

Pore compressibility is an important parameter in reservoir engineering. However, its variation from laboratory core analysis or logging data can be large. Moreover, laboratory core analysis cannot identify the influence of macroscopic fractures on pore compressibility. The geological reserves obtained with the commonly used flowing material balance (FMB) method are significantly impacted by the accuracy of the pore compressibility. Therefore, a new form of the FMB method is proposed in this study which can determine the pore compressibility and geological reserves at the same time. For gas wells, the new method uses the material balance equation and the FMB equation including the pore compressibility. For oil wells, new forms of the material balance equation and the FMB equation were established which have the same form as the corresponding equations for gas wells. A new linear expression of the material balance equation is employed for the analysis. Simulation results indicate that the new method can provide more precise predictions of both the pore compressibility and the geological reserves. Furthermore, the new method also considers the influence of formation fractures because it uses well production data. Sensitivity analysis indicates that the error in the pore compressibility has a significant influence on the determination of the geological reserves.

1. Introduction

Pore compressibility is the change in rock pore volume with varying pore pressure, and it is a fundamental parameter of the flow equations for porous media. Pore compressibility is used in well testing, rate transient analysis, material balance, and reservoir simulations (Iwere et al., 2002; Haynes et al., 2008; Tonnsen and Miskimins, 2011; Lan et al., 2017). In 1953, Hall (1953) developed an empirical chart for pore compressibility with porosity from experimental results of limestone and sandstone cores. Later, the compressibility of different types of sandstone, carbonate, and consolidated and unconsolidated rocks were also investigated (Newman, 1973; Pauget et al., 2002; Jalalh, 2006a, 2006b; Zaki et al., 1995; Chertov and Suarez-Rivera, 2014; Oliveira et al., 2016).

It has been determined that pore compressibility is influenced by the stress state, stress path (Von Gonten and Choudhary, 1969; Lachance and Andersen, 1983; Hettema et al., 2000; Yi et al., 2005; Carvajal et al., 2010), and fluid properties (Carles and Lapointe, 2005). In addition to the direct measurement method for pore compressibility, many indirect evaluation methods have also been proposed which relate the pore compressibility to other mechanical parameters (Sampath, 1982; Zimmerman, 1991; Bai et al., 2010; Saxena, 2011; Hettema et al., 2013; Zeng and Wang, 2017). Using these methods, pore compressibility can be evaluated from core analysis or logging data (Khatchikian, 1996; Seehong et al., 2001; Wolf et al., 2005; Oliveira et al., 2014). Several other evaluation methods have also been proposed. For example, Ling et al. (2014) and He et al. (2016) developed a method to determine pore compressibility through permeability experiments. Siddiqui et al. (2010) used computed tomography (CT) scanning to evaluate the pore compressibility.

At this point, pore compressibility is mainly investigated using core analysis, empirical equations, and logging data. However, the experimental determination of compressibility faces the problem of heterogeneity, and cores cannot reflect the influence of macroscopic fractures. Although logging data describes a larger sample of the reservoir, it still only represents the properties of the volume near the well. To obtain a parameter that reflects the average property of the well drainage volume, a new evaluation method for pore compressibility is needed. The

* Corresponding author.
E-mail address: liuyuewulxs@126.com (Y. Liu).

https://doi.org/10.1016/j.petrol.2018.09.010
Received 12 June 2018; Received in revised form 31 August 2018; Accepted 4 September 2018
Available online 06 September 2018

feedback control methods can be used to investigate the spatial variation of reservoir state and properties, but the algorithms are complicated (Narasingam et al., 2018; Siddhamshetty and Kwon, 2018).

Production data reflects the average properties of the well drainage volume, and it is an important input parameter for the flowing material balance (FMB) method that is commonly used to evaluate geological reserves. In fact, this method obtains the product of geological reserves and pore compressibility by linear fitting, in which the pore compressibility plays an important role. Therefore, the pore compressibility is critical for accurate evaluation of geological reserves (see section 5.1 for details). In this study, a new method to determine the pore compressibility is proposed based on the FMB method in order to obtain more accurate evaluation of geological reserves.

2. FMB method

2.1. FMB equation for gas wells

The FMB equation for gas reservoirs used in this study is very similar to that reported in the literature; however, the proposed FMB equation for oil reservoirs is quite different from that in the literature. For completeness of the discussion and to facilitate understanding of the FMB equation for oil reservoirs proposed in this paper, the derivation of the FMB equation for gas reservoirs is also presented in detail. In the literature, pore compressibility and irreducible water saturation are neglected in the FMB equation for gas reservoirs (Mattar and McNeil, 1998; Sun, 2015). In this study, an equation considering the pore compressibility is derived. For a closed dry gas reservoir with irreducible water, the material balance equation is as follows (Dake, 2004):

$$GB_{gi} = (G - G_p)B_g + GB_{gi}\left(\frac{C_w S_{wi} + C_f}{1 - S_{wi}}\right)\Delta p \tag{1}$$

$$\Delta p = p_i - p \tag{2}$$

where G is the gas initially in place (m^3), G_p is the cumulative produced gas (m^3), B_{gi} is the original gas formation volume factor (m^3/m^3), B_g is the gas formation volume factor (m^3/m^3), S_{wi} is the initial water saturation (%), C_w is the formation water compressibility (MPa^{-1}), C_f is the pore compressibility (MPa^{-1}), p_i is the original formation pressure (MPa), p is the formation pressure (MPa), and the subscript i indicates the original formation state.

Therefore,

$$G = \frac{G_p B_g}{(B_g - B_{gi}) + B_{gi}\left(\frac{C_w S_{wi} + C_f}{1 - S_{wi}}\right)\Delta p} \tag{3}$$

where

$$B_g = \frac{p_{sc} Z T}{p T_{sc}} \quad B_{gi} = \frac{p_{sc} Z_i T_i}{p_i T_{sc}} \tag{4}$$

in which T is the formation temperature (K), T_{sc} is the temperature at the standard condition (K), p_{sc} is the pressure at the standard condition (MPa), Z is the gas deviation factor, Z_i is the initial gas deviation factor, and the subscript sc indicates the standard condition.

The effective compressibility is defined as follows:

$$C_e = \frac{C_w S_{wi} + C_f}{1 - S_{wi}} \tag{5}$$

Eq. (5) reflects the effect of the compressibility of irreducible water, and it would be the pore compressibility when there is no water. Substituting Eqs. (4) and (5) into Eq. (3), the following expression can be obtained:

$$\left(1 - \frac{G_p}{G}\right)\frac{p_i}{Z_i} = \frac{p}{Z}(1 - C_e \Delta p) \tag{6}$$

Taking the derivative of the two sides of Eq. (6) with respect to time yields the following:

$$q = -\frac{GZ_i p}{Zp_i}[C_g(1 - C_e\Delta p) + C_e]\frac{dp}{dt} = -\frac{GZ_i p}{Zp_i(1 - S_{wi})}C_t\frac{dp}{dt} \tag{7}$$

where q is the gas production rate (m^3/s), t is the time (s), C_g is the gas compressibility (MPa^{-1}), and ρ is the gas density (kg/m^3). The total compressibility is expressed as follows:

$$C_t = C_w S_{wi} + C_f + C_g(1 - S_{wi}) - C_g(C_w S_{wi} + C_f)\Delta p \tag{8}$$

The gas compressibility can be expressed as follows:

$$C_g = \frac{1}{\rho}\frac{d\rho}{dp} = \frac{ZRT}{pM_g}\frac{d}{dp}\left(\frac{pM_g}{ZRT}\right) = \frac{Z}{p}\frac{d}{dp}\left(\frac{p}{Z}\right) \tag{9}$$

The following real gas state equation is used in Eq. (9):

$$\rho = \frac{pM_g}{ZRT} \tag{10}$$

where M_g is the gas molecular molar mass (kg/mol), and R is the universal gas constant, 8.314 J/(mol·K).

The normalized pseudo-pressure can be defined as follows:

$$p_p = \left(\frac{\mu_g Z}{p}\right)_i \int_0^p \frac{p}{\mu_g Z}dp \tag{11}$$

where μ_g is the gas viscosity (Pa·s).

The material balance pseudo-time is defined as follows:

$$t_{ca} = \frac{(\mu_g C_t)_i}{q}\int_0^t \frac{q}{\mu_g C_t}dt \tag{12}$$

Substituting Eq. (7) and the normalized pseudo-pressure definition in Eq. (11) into the MB pseudo-time definition in Eq. (12) yields the following:

$$t_{ca} = -\frac{G}{q(1 - S_{wi})}\left(\frac{\mu_g Z C_t}{p}\right)_i \int_{p_i}^{p} \frac{p}{\mu_g Z}dp = \frac{GC_{ti}}{q(1 - S_{wi})}(p_{p_i} - p_p) \tag{13}$$

That is:

$$\frac{p_{p_i} - p_p}{q} = \frac{t_{ca}(1 - S_{wi})}{GC_{ti}} \tag{14}$$

Considering the formation irreducible water, the continuity equation describing the flow in porous media for gas reservoir is as follows:

$$\frac{\partial(\rho\phi_e)}{\partial t} + \nabla\cdot(\rho V) = 0 \tag{15}$$

where

$$\phi_e = \phi_i[1 - S_{wi} - (C_w S_{wi} + C_f)\Delta p] \tag{16}$$

$$V = -\frac{K}{\mu_g}\nabla p \tag{17}$$

in which ϕ_e is the effective porosity (%), V is the flow velocity in porous media (m/s), K is the permeability (m^2), and ϕ_i is the initial porosity (%).

Substituting Eqs. (10) and (17) into Eq. (15) yields the following:

$$\nabla\cdot\left(\frac{pM_g}{ZRT}\frac{K}{\mu_g}\nabla p\right) = \frac{\partial}{\partial t}\left(\phi_e\frac{pM_g}{ZRT}\right) \tag{18}$$

Assuming the formation is isothermal, Eq. (18) becomes

$$\nabla\cdot\left(\frac{p}{Z}\frac{K}{\mu_g}\nabla p\right) = \frac{\partial}{\partial t}\left(\phi_e\frac{p}{Z}\right) \tag{19}$$

Assuming the permeability, K, is constant, and using the definition of normalized pseudo-pressure in Eq. (11), the left side of Eq. (19) becomes

$$\nabla\cdot\left(\frac{p}{Z}\frac{K}{\mu_g}\nabla p\right)=K\left(\frac{p}{\mu_g Z}\right)_i\nabla^2 p_p \tag{20}$$

Using Eq. (10) and the definitions of the total compressibility in Eq. (8), the normalized pseudo-pressure in Eq. (11), and the material balance pseudo-time in Eq. (12), the right side of Eq. (19) can be expressed as follows:

$$\begin{aligned}\frac{\partial}{\partial t}\left(\phi_e\frac{p}{Z}\right)&=\frac{p}{Z}\frac{d\phi_e}{dp}\frac{\partial p}{\partial t}+\phi_e\frac{d}{dp}\left(\frac{p}{Z}\right)\frac{\partial p}{\partial t}\\&=\frac{p}{Z}\phi_i(C_wS_{wi}+C_f)\frac{\partial p}{\partial t}+C_g\phi_e\frac{p}{Z}\frac{\partial p}{\partial t}\\&=C_t\phi_i\frac{p}{Z}\frac{\partial p}{\partial t}=(\phi\mu_g C_t)_i\left(\frac{p}{\mu_g Z}\right)_i\frac{\partial p_p}{\partial t_{ca}}\end{aligned} \tag{21}$$

Using Eqs. (20) and (21), Eq. (19) can be written as follows:

$$\nabla^2 p_p=\frac{(\phi\mu C_t)_i}{K}\frac{\partial p_p}{\partial t_{ca}} \tag{22}$$

Equation (22) has the same form as the seepage equation for a weak compressible fluid. For a gas well with a constant production rate, when the reservoir is in pseudo-steady state, the following expression can be applied (Sun, 2015):

$$\frac{p_p-p_{p_{wf}}}{q}=\frac{(\mu B)_i}{2\pi Kh}\left[\frac{1}{2}\ln\left(\frac{4A}{C_A e^{\gamma}r_{aw}^2}\right)\right]=b_{a,pss} \tag{23}$$

where p_{wf} is the bottom hole pressure (MPa), h is the reservoir thickness (m), $\boldsymbol{A}$ is the reservoir area (m^3), C_A is the shape factor (Dietz, 1965), γ is Euler's constant, $r_{aw}=r_w e^{-s}$ is the effective well radius (m), r_w is the well radius (m), and s is the skin factor.

Using Eqs. (14) and (23) yields the following:

$$\frac{p_{p_i}-p_{p_{wf}}}{q}=\frac{(\mu B)_i}{4\pi Kh}\ln\left(\frac{4A}{C_A e^{\gamma}r_{aw}^2}\right)+\frac{t_{ca}(1-S_{wi})}{GC_{ti}} \tag{24}$$

Equation (24) is the gas well FMB equation considering the pore compressibility.

2.2. FMB equation for oil wells

Pore compressibility cannot be determined by the conventional FMB method for oil wells owing to the oversimplification in the common material balance equation, i.e., assuming the oil formation volume factor is constant. When the oil formation volume factor is variable, a new form of the material balance equation and the FMB equation thus need to be established.

For a closed unsaturated oil reservoir without producing water, it holds that (Dake, 1978):

$$NB_{oi}=(N-N_p)B_o+\frac{NB_{oi}}{1-S_{wi}}(C_wS_{wi}+C_f)\Delta p \tag{25}$$

where N is the oil initially in place (m^3), N_p is the cumulative producing gas (m^3), B_{oi} is the original oil formation volume factor (m^3/m^3), B_o is the oil formation volume factor (m^3/m^3), N_p is the cumulative oil production (m^3), and $\Delta p=p_i$-p is the formation pressure drop (MPa).

Using Eq. (4), Eq. (25) can be written as follows:

$$\frac{1}{B_o}(1-C_e\Delta p)=\frac{1}{B_{oi}}\left(1-\frac{N_p}{N}\right) \tag{26}$$

This equation has the same form as the gas reservoir material balance in Eq. (6). Taking the derivative of both sides of Eq. (26) with respect to time yields the following expression:

$$\frac{1}{dt}\left[\frac{1}{B_o}(1-C_e\Delta p)\right]=-\frac{q}{NB_{oi}} \tag{27}$$

The right side of Eq. (27) can be expressed as follows:

$$\begin{aligned}&\frac{1}{dt}\left[\frac{1}{B_o}(1-C_e\Delta p)\right]\\&=\left(1-\frac{C_wS_{wi}+C_f}{1-S_{wi}}\Delta p\right)\frac{C_o}{B_o}\frac{dp}{dt}+\frac{1}{B_o}\frac{C_wS_{wi}+C_f}{1-S_{wi}}\frac{dp}{dt}\\&=\frac{C_t^*}{B_o(1-S_{wi})}\frac{dp}{dt}\end{aligned} \tag{28}$$

Therefore, Eq. (27) can be written as the following:

$$q=-\frac{NB_{oi}}{B_o(1-S_{wi})}C_t^*\frac{dp}{dt} \tag{29}$$

where

$$C_t^*=(1-S_{wi})C_o-(C_wS_{wi}+C_f)C_o\Delta p+C_wS_{wi}+C_f \tag{30}$$

For oil reservoirs, using Eq. (16), the first term of the continuity equation in Eq. (15) becomes the following:

$$\begin{aligned}\frac{\partial(\rho\phi_e)}{\partial t}&=\frac{\partial}{\partial t}\left\{\frac{\rho_{sc}}{B_o}\phi_i[1-S_{wi}+(C_wS_{wi}+C_f)\Delta p]\right\}\\&=\rho_{sc}\phi_i(1-S_{wi})\frac{\partial}{\partial t}\left[\frac{1}{B_o}\left(1+\frac{C_wS_{wi}+C_f}{1-S_{wi}}\Delta p\right)\right]\\&=\frac{\rho_{sc}\phi_i C_t^*}{B_o}\frac{\partial p}{\partial t}\end{aligned} \tag{31}$$

The second term of the continuity equation given in Eq. (15) is as follows:

$$\begin{aligned}\nabla\cdot(\rho V)&=\frac{1}{r}\frac{\partial}{\partial r}\left(-r\rho\frac{K}{\mu_o}\frac{\partial p}{\partial r}\right)=-\frac{1}{r}\frac{\partial}{\partial r}\left(r\frac{\rho_{sc}}{B_o}\frac{K}{\mu_o}\frac{\partial p}{\partial r}\right)\\&=-\frac{\rho_{sc}K}{r}\frac{\partial}{\partial r}\left(r\frac{1}{B_o\mu_o}\frac{\partial p}{\partial r}\right)\end{aligned} \tag{32}$$

The normalized pseudo-pressure for oil wells is defined as follows:

$$p_p^*=(B_o\mu_o)_i\int_0^p\frac{1}{B_o\mu_o}dp \tag{33}$$

The material balance pseudo-time for oil wells is defined as:

$$t_{ca}^*=\frac{(\mu_oC_t^*)_i}{q}\int_0^t\frac{q}{\mu_oC_t^*}dt \tag{34}$$

Using Eqs. (31)–(34), the governing equation of the flow in porous media for oil wells is as follows:

$$\nabla^2p_p^*=\frac{(\phi\mu_oC_t^*)_i}{K}\frac{\partial p_p^*}{\partial t_{ca}^*} \tag{35}$$

Equation (35) has the same form as Eq. (22), while Eq. (26) has the same form as Eq. (6). Therefore, the same form of the FMB equation as in Section 2.1 can be obtained.

3. Evaluation method for pore compressibility and geological reserves

3.1. Proposed new method

When the total compressibility and initial water saturation is known, the gas initially in place (GIIP) can be determined by linear regression using the FMB equations. If the pore compressibility is unknown, it cannot be directly obtained with the commonly used equations. As the FMB equations for oil and gas wells have the same form, the gas well equation is taken as an example. The following are first defined:

$$\varphi=\frac{p/Z}{p_i/Z_i} \tag{36}$$

$$X_G=\frac{G_p}{\varphi\Delta p}\ Y_p=\frac{1-\varphi}{\varphi\Delta p} \tag{37}$$

Then, Eq. (6) can be written as follows:

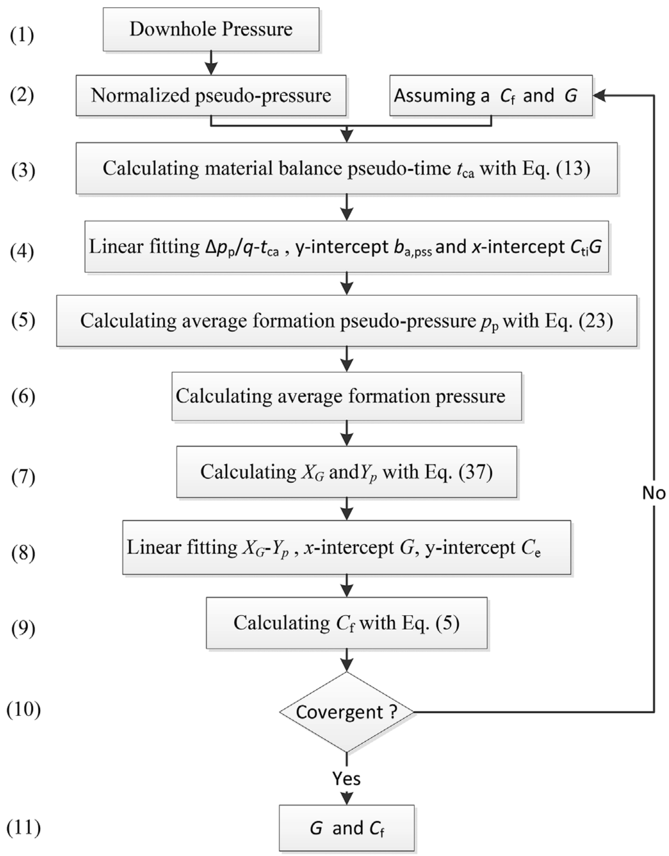

Fig. 1. Workflow of the proposed new FMB method.

$$Y_p = -C_e + \frac{1}{G}X_G \tag{38}$$

For oil wells, N, N_p, and X_N are used in place of G, G_p, and X_G, respectively. in Eqs. (37) - (38), Eq. (39) is used instead of Eq. (36).

$$\varphi = \frac{B_{oi}}{B_o} \tag{39}$$

Therefore, when the pore compressibility is unknown, the pore compressibility and GIIP can be evaluated together by following the workflow shown in Fig. 1. In Fig. 1, C_f, which is calculated in line 9, can also be obtained using the values for GC_{ti} determined in line 4 and G in line 8, or by using G obtained from Eq. (6) and C_f in line 4.

There are three main differences between the proposed FMB method and the commonly used FMB method: the proposed new FMB equation for gas wells considers the pore compressibility, the new equation for oil wells has the same form as that for gas wells, and the material balance equation can be used for a linear regression to obtain the two parameters together.

3.2. Comparisons

A comparison between the proposed new method and the conventional method is given in Table 1. While the conventional method only needs to fit the FMB equation, the new method needs to fit both the FMB equation and the material balance equation. In addition, the conventional method assumes that the pore compressibility is known and only the geological reserves need to be obtained; the new method considers both the pore compressibility and the geological reserves to be unknown, and these two parameters can be obtained at the same time. Regarding the solution methods, the conventional FMB equation for oil wells can directly fit the geological reserves and does not need to be solved iteratively. When fitting the conventional FMB equation for gas wells, only a geological reserve needs to be assumed. For the new method, both the FMB equations for oil and gas wells need to assume a geological reserve and pore compressibility, and these two parameters are iteratively solved for simultaneously. Furthermore, the conventional FMB equation for oil wells uses pressure and time, while the new method uses pseudo-pressure and material balance pseudo-time. Another small difference is that the conventional FMB equations do not explicitly consider water saturation.

4. Gas and oil reservoir cases

4.1. Gas reservoir case

An example of the production data for a gas well is simulated in this section. The simulation method is presented in the appendix. The simulation parameters are listed in Table 2. The actual GIIP calculated using the volume method is $G = \phi(1\text{-}S_{wi})\pi r_e^2 hB_{gi} = 1.373 \times 10^9\,\text{m}^3$. The simulated results are shown in Fig. 2.

Assuming the pore compressibility $C_f = 1.0 \times 10^{-3}\,\text{MPa}^{-1}$, and the GIIP $G = 3.0 \times 10^9\,\text{m}^3$, the normalized pseudo-pressure and material balance pseudo-time were calculated using the simulated production data. This data was then fitted with the line $\Delta p_p/q$-$(1\text{-}S_{wi})t_{ca}$, and the results are shown in Fig. 3. Next, the computed $b_{a,pss}$ was used to calculate the average formation pressure, after which $(1\text{-}\varphi)/\varphi\Delta p$ and $G_p/\varphi\Delta p_p$ were computed and fitted, as shown in Fig. 4. The results are $C_e = 2.59 \times 10^{-3}\,\text{MPa}^{-1}$ and $G = 1.368 \times 10^9\,\text{m}^3$. Using Eq. (5), the pore compressibility $C_f = 2.02 \times 10^{-3}\,\text{MPa}^{-1}$. The calculations in the first iteration are listed in Table 3. The results show that the GIIP and pore compressibility computed by the proposed new method are close to the actual values. If more accurate results are required, the iterations can be continued. If a pore compressibility $C_f = 1.0 \times 10^{-3}\,\text{MPa}^{-1}$ is used, the resulting GIIP calculated using the conventional method is $1.733 \times 10^9\,\text{m}^3$, which represents an error of 26.2%.

4.2. Oil reservoir case

An example of the production data for an oil well is simulated in this section. The simulation parameters are listed in Table 4. The actual oil initially in place (OIIP) calculated with the volume method is $N = \phi(1\text{-}S_{wi})\pi r_e^2 hB_{oi} = 1.003 \times 10^6\,\text{m}^3$. The simulated results are shown in Fig. 5.

Assuming a pore compressibility $C_f = 5.0 \times 10^{-4}\,\text{MPa}^{-1}$ and an OIIP $N = 2.0 \times 10^6\,\text{m}^3$, the normalized pseudo-pressure and material balance pseudo-time were calculated using the simulated production data. This data was fitted with the line $\Delta p_p/q$-$(1\text{-}S_{wi})t_{ca}$, and the results are shown in Fig. 6. Next, the computed $b_{a,pss}$ was used to calculate the average formation pressure, and $(1\text{-}\varphi)/\varphi\Delta p$ and $N_p/\varphi\Delta p_p$ were then computed and fitted, as shown in Fig. 7. The results are $Ce = 1.36 \times 10^{-3}\,\text{MPa}^{-1}$, and $N = 1.004 \times 10^6\,\text{m}^3$. Using Eq. (5), the pore compressibility $C_f = 1.003 \times 10^{-3}\,\text{MPa}^{-1}$. The first iteration calculation results are listed in Table 5, and demonstrate that the OIIP and pore compressibility computed using the proposed new method are close to the actual values. If more accurate results are required, the iterations can be continued. If a pore compressibility $C_f = 5.0 \times 10^{-3}\,\text{MPa}^{-1}$ is used, the resulting OIIP calculated using the conventional method is $1.23 \times 10^6\,\text{m}^3$, which represents an error of 22.8%.

As it can be seen from the above cases, the proposed method has high computational efficiency. Although it is not mathematically proved that the method can obtain a global optimum, experience and geological knowledge are beneficial for giving appropriate initial values. When the guess value is far from the true one, the pseudo-steady state segment becomes a curve. These can help to get reasonable values in practice.

Table 1
Comparison between the conventional and proposed new methods.

	conventional method		new method	
	oil wells (Sun, 2015)	gas wells (Sun, 2015)	oil wells	gas wells
FMB	$\frac{\Delta p}{q} = b_{pss} + \frac{t}{NC_t}$	$\frac{\Delta p_p}{q} = b_{a,pss} + \frac{t_{ca}}{GC_{ti}}$	$\frac{\Delta p_p}{q} = b_{a,pss} + \frac{t_{ca}(1-S_{wi})}{GC_{ti}}$	$\frac{\Delta p_p}{q} = b_{a,pss} + \frac{t_{ca}(1-S_{wi})}{NC_{ti}}$
material balance	/	/	$Y_p = -C_e + \frac{1}{G}X_G$	$Y_p = -C_e + \frac{1}{N}X_N$
iteration	/	G	G, C_f	N, C_f
results	N	G	G, C_f	N, C_f

Table 2
Gas reservoir simulation parameters.

reservoir thickness (m)	permeability (mD)	initial pressure (MPa)	irreducible water saturation	gas relative density	porosity
50	10	100	0.2	0.6	10%
formation temperature (°C)	skin factor	well radius (m)	pore compressibility (MPa^{-1})	formation water specific	GIIP (m^3)
100	0	0.1	2.0×10^{-3}	1.008	1.373×10^9

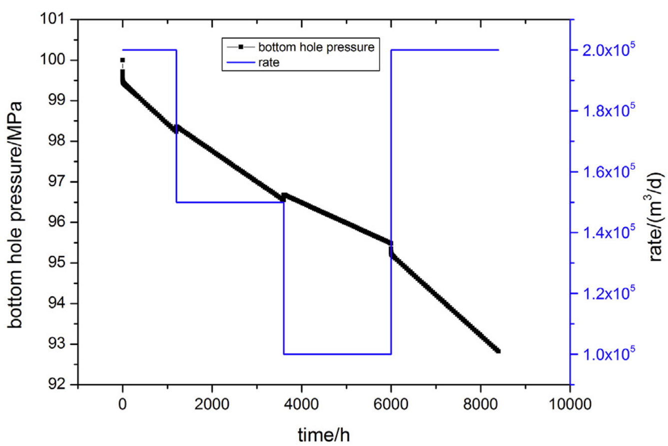

Fig. 2. Simulated gas production history.

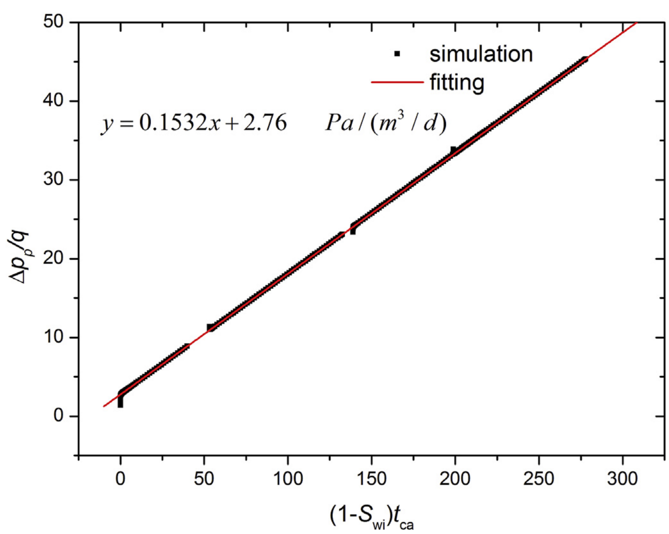

Fig. 3. Fitting to $\Delta p_p/q$-$(1\text{-}S_{wi})t_{ca}$ for the gas reservoir.

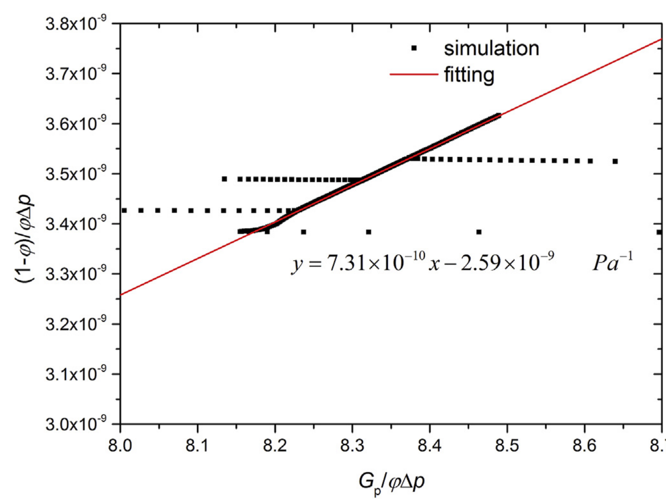

Fig. 4. Fitting to $(1\text{-}\varphi)/\varphi\Delta p$-$G_p/\varphi\Delta p_p$ for the gas reservoir.

5. Discussion

5.1. Influence of pore compressibility

If the pore compressibility is not accurate, the geological reserve determined using the FMB method will not be accurate either. Based on the parameters for the examples in Section 4, the error in the geological reserve with the pore compressibility error is analyzed in Figs. 8–11 under different formation pressures, temperatures, pore compressibilities, and irreducible water saturations. The pore compressibility ratio is defined as the ratio of the pore compressibility used in the FMB method to the actual pore compressibility. The results show that the influence of the pore compressibility error on the geological reserve increases with the initial formation pressure, irreducible water saturation, and pore compressibility, and decreases with the formation temperature. The formation temperature and irreducible water saturation have little impact on the error in the geological reserves. If the pore compressibility differs from the actual value by an order of magnitude, an error of approximately 20–80% in the geological reserves may result.

Table 3
First iteration of the computation for the gas reservoir.

Assumption		$C_{ti}G$ (m^3/Pa)	$b_{a,pss}$ (Pa/(m^3/d))	Ce (MPa^{-1})	Iteration results	
C_f (MPa^{-1})	G (m^3)				C_f (MPa^{-1})	G (m^3)
1.0×10^{-3}	3.0×10^9	6.5274	2.76	2.59×10^{-3}	2.02×10^{-3}	1.368×10^9

Table 4
Oil reservoir simulation parameters.

reservoir thickness (m)	permeability (mD)	initial pressure (MPa)	irreducible water saturation	porosity	
20	10	30	0.2	10%	
formation temperature (°C)	skin factor	well radius (m)	pore compressibility (MPa^{-1})	formation water specific	OIIP (m^3)
60	0	0.1	1.0×10^{-3}	1.008	1.003×10^6

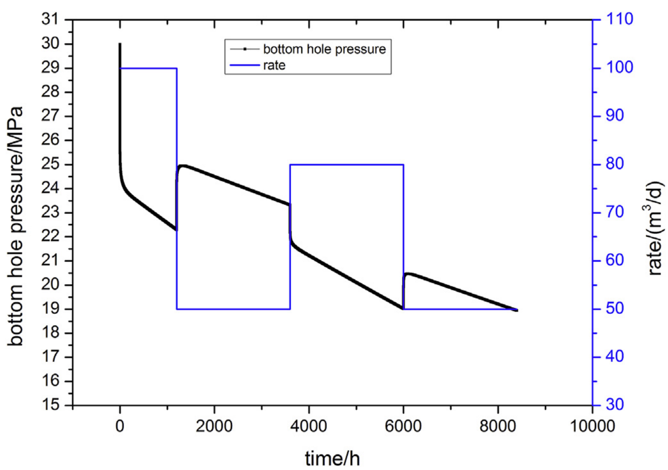

Fig. 5. Simulated oil production history.

Therefore, the pore compressibility has a significant impact on the geological reserves obtained using the FMB method, particularly when the formation pressure is very high. Because the oil compressibility is small relative to the gas compressibility, and is closer to the pore compressibility, the pore compressibility has a more significant influence on the evaluated geological reserves of oil reservoirs.

5.2. Applicability

In the derivation, the permeability is assumed to be constant, but this assumption is unnecessary in practical. The second term on the right side of Eq. (24) is determined by the material balance equation and is not affected by changes in permeability. The first item on the right side is determined by the permeability of the reservoir, the reservoir geometry shape and the location of the well. The specific form would be obtained based on the permeability spatial distribution. However, as it can be seen from the workflow in Fig. 1, the specific expression of $b_{a,\ pss}$ is not required Therefore, the proposed method is also applicable to cases with spatial variation of permeability. However, it should be pointed out that the pore compressibility obtained in this method is the average within the well drainage volume.

The new method is proposed for the single-phase flow of dry gas reservoirs and unsaturated oil reservoirs that do not produce water. Only the elastic expansion and rock pore compaction are considered as driving mechanisms. In practice, oil or gas well production may be a multiphase flow, e.g., a water/oil flow, water/gas flow, or oil/gas flow. Actual reservoir production may also have other driving mechanisms, such as water drive, dissolved gas drive, and gas top drive. For weak consolidated rocks, rock compaction is strong, and the formation permeability will change significantly with a decrease in pressure. Here, a constant permeability is assumed during the production process. Hence, the proposed method is only applicable for analysis of a short production period of consolidated reservoirs. Therefore, there is still a need to develop additional methods that are suitable for these situations.

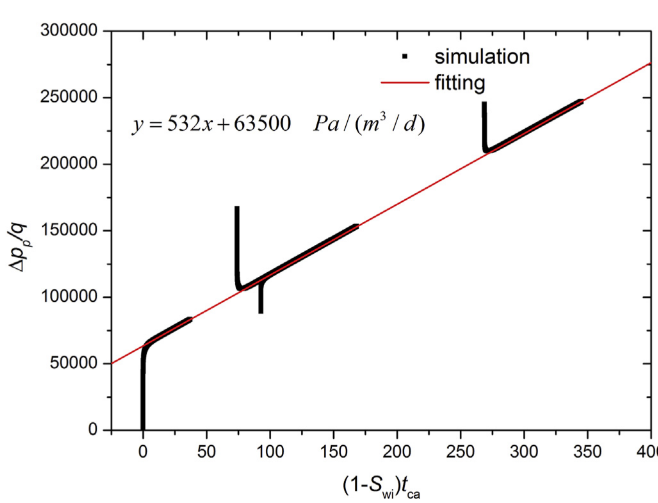

Fig. 6. Fitting to $\Delta p_p/q$-$(1\text{-}S_{wi})t_{ca}$ for the oil reservoir.

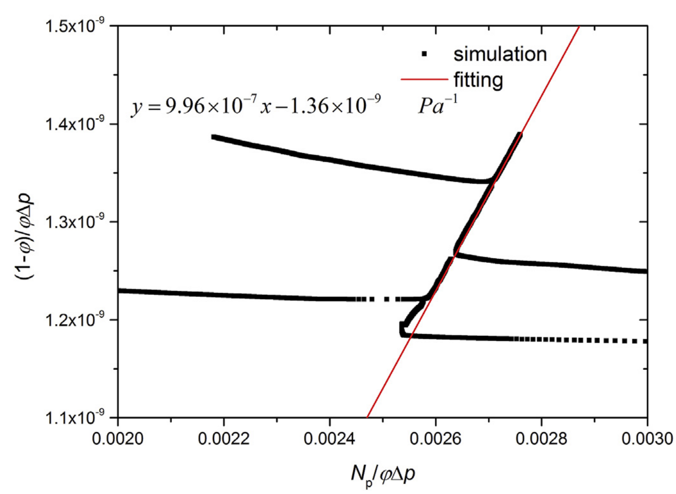

Fig. 7. Fitting to $(1\text{-}\varphi)/\varphi\Delta p$-$N_p/\varphi\Delta p_p$ for the oil reservoir.

Table 5
First iteration of the computation for the oil reservoir.

Assumption		$C_{ti}N$ (m^3/Pa)	$b_{a,pss}$ (Pa/(m^3/d))	Ce (MPa^{-1})	Iteration results	
C_f (MPa^{-1})	N (m^3)				C_f (MPa^{-1})	N (m^3)
5.0×10^{-4}	2.0×10^{6}	1.88×10^{-3}	63500	1.36×10^{-3}	1.003×10^{-3}	1.004×10^{6}

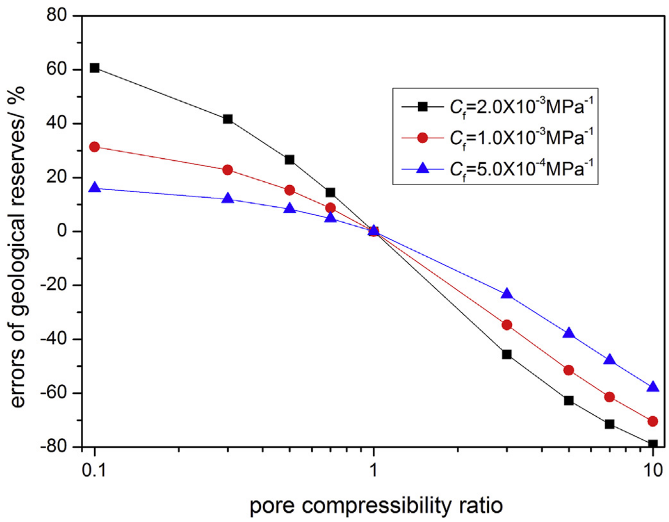

Fig. 8. Influence of the pore compressibility on error in the geological reserves.

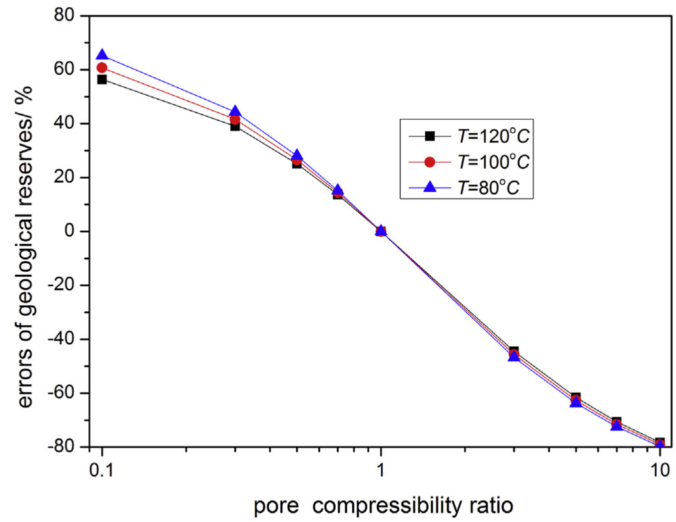

Fig. 10. Influence of the formation temperature on error in the geological reserves.

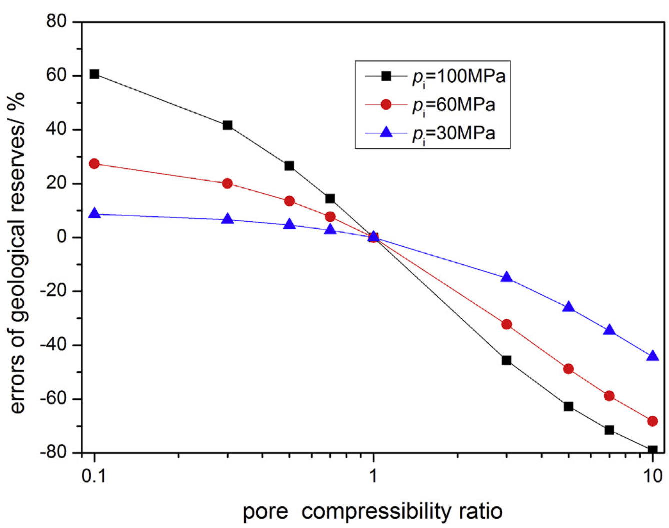

Fig. 9. Influence of the initial formation pressure on error in the geological reserves.

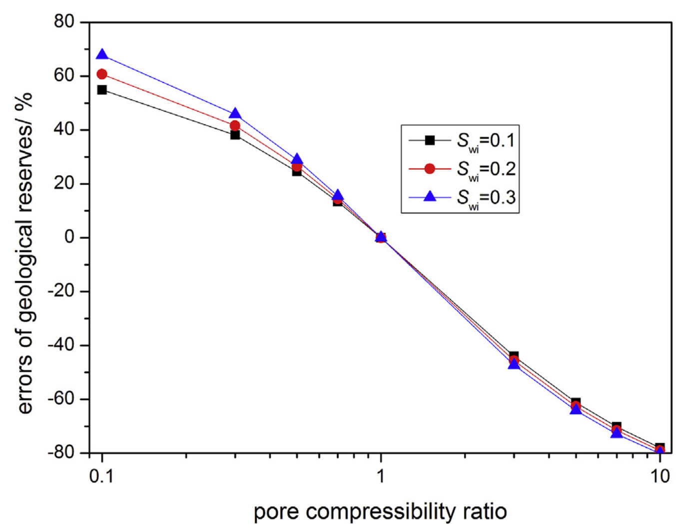

Fig. 11. Influence of the irreducible water saturation on error in the geological reserves.

6. Conclusions

Pore compressibility determined by core analysis and logging data is poorly representative, and thus cannot reflect the overall reservoir properties. This uncertainty in the pore compressibility can result in significant error in the evaluation of geological reserves using the FMB equation. In this paper, a new FMB equation considering pore compressibility was established for gas wells. For oil wells, the commonly used material balance equation and FMB equation were transformed into the same form as these for gas wells. Based on the FMB method, a new linear regression equation for the material balance equation was proposed, which can be used to obtain the geological reserves and pore compressibility at the same time. The results of simulated example cases indicate that the proposed method can provide more accurate values for the geological reserve and pore compressibility. Impact factor analyses indicate that the error in the pore compressibility has a significant influence on the geological reserve calculated using the FMB method.

Acknowledgments

The first authors acknowledge the National Natural Science Foundation of China (Grant No.11602276) for the financial support to this research.

Appendix. Simulation method

For simplicity, only an oil or gas reservoir with a circular boundary and a centered wellbore is considered. The oil production can be described by the governing equations in a cylindrical coordinate system as follows:

$$\frac{C_t^* \phi_i}{B_o}\frac{\partial p}{\partial t} = \frac{1}{r}\frac{\partial}{\partial r}\left(r\frac{k}{B_o \mu_o}\frac{\partial p}{\partial r}\right) \tag{A-1}$$

The initial condition is as follows:

$$p(r, 0) = p_i \tag{A-2}$$

The interior boundary condition is defined as follows:

$$2\pi r_w h \frac{k}{\mu_o}\frac{\partial p}{\partial r}\bigg|_{r=r_w} = C\frac{dp_w}{dt} + B_o q \tag{A-3}$$

The outer boundary condition is given by the following:

$$\frac{\partial p}{\partial r}\bigg|_{r=r_e} = 0 \tag{A-4}$$

In addition:

$$p|_{r=r_w} = p_w + \frac{q\mu B_o S}{2\pi kh} \tag{A-5}$$

where C is the wellbore storage coefficient (m^3/Pa). For gas reservoirs, C_o, B_o, and μ_o are replaced with C_g, B_g, and μ_g, respectively, in the above formulae.

If $r = r_w e^x$, the governing equation in Eq. (A-1) and boundary conditions in Eqs. (A-3) to (A-5) can be rewritten, respectively, as follows:

$$r_w^2 e^{2x}\frac{C_t^* \phi_i}{B_o}\frac{\partial p}{\partial t} = \frac{\partial}{\partial x}\left(\frac{k}{B_o \mu_o}\frac{\partial p}{\partial x}\right) \tag{A-6}$$

$$\frac{2\pi r_w hk}{r_w e^x \mu_o}\frac{\partial p}{\partial x}\bigg|_{x=0} = C\frac{dp_w}{dt} + B_o q \tag{A-7}$$

$$\frac{\partial p}{\partial x}\bigg|_{x=\ln(r_e/r_w)} = 0 \tag{A-8}$$

For convenience, the following are defined:

$$A = r_w^2 e^{2x}\frac{C_t^* \phi_i}{B_o},\ B = \frac{k}{B_o \mu_o},\ E = \frac{2\pi r_w hk}{r_w e^x \mu_o} \tag{A-9}$$

Dividing the reservoir into N segments along the radial direction, and taking the equidistant grid $\Delta x = \ln\left({}^{r_e}/_{r_w}\right)/N$, Eqs. (A-6)–(A-8) can be discretized into the following forms, respectively:

$$A_j^s \frac{p_j^{(s+1)} - p_j^n}{\Delta t} = \frac{1}{\Delta x_j}\left(B_{j+\frac{1}{2}}^{(s)}\frac{p_{j+1}^{(s+1)} - p_j^{(s+1)}}{\Delta x_{j+\frac{1}{2}}} - B_{j-\frac{1}{2}}^{(s)}\frac{p_j^{(s+1)} - p_{j-1}^{(s+1)}}{\Delta x_{j-\frac{1}{2}}}\right) \tag{A-10}$$

$$E_0^s \frac{p_1^{(s+1)} - p_{-1}^{(s+1)}}{\Delta x_0}\Bigg|_{x=0} = C^{(s)}\frac{p_w^{(s+1)} - p_w^n}{\Delta t} + B_o q^{(s)} \tag{A-11}$$

$$\frac{p_{N+1}^{(s+1)} - p_{N-1}^{(s+1)}}{\Delta x_N} = 0 \tag{A-12}$$

where Δt is the time step, superscript n denotes the nth time step, and s denotes the sth iteration of a time step. Because the coefficients A, B, C, and E are all functions of pressure, and the difference equations are nonlinear, in order to linearly solve the difference equation, the values of the sth iterative step are used for A, B, C and E in the $(s+1)$th iteration of each time step. Thus, the difference equations can be solved iteratively.

References

Bai, M., Shen, X., Li, G., 2010. Alternative method to determine pore volume compressibility attributable to production-induced reservoir compaction. In: SPE Paper 130212 Presented at the International Oil and Gas Conference and Exhibition in China, Beijing, China, 8-10 June.

Carles, P., Lapointe, P., 2005. Water-weakening of carbonates under stress, new insights into pore-volume compressibility measurements. Petrophysics 46 (5), 361–368.

Carvajal, J.M., Saavedra, N.F., Calderon, Z.H., 2010. Stress effect on compressibility of weakly anisotropic micro-fractured rocks a study case on Colombian foothills tight sandstones. In: ARMA Paper 10-474 Presented at the 44th U.S. Rock Mechanics Symposium and 5th U.S.-Canada Rock Mechanics Symposium, Salt Lake City, Utah, 27-30 June.

Chertov, M.A., Suarez-Rivera, R., 2014. Practical laboratory methods for pore volume compressibility characterization in different rock types. In: AEMA Paper 14-7532 Presented at the 48th U.S. Rock Mechanics/Geomechanics Symposium, Minneapolis, Minnesota, pp. 1–4 (June).

Dake, L.P., 1978. Fundamentals of Reservoir Engineering. Elsevier Scientific Publishing Company, Amsterdam-Oxford-New York.

Dake, L.P., 2004. The Practice of Reservoir Engineering, revised edition. Elsevier Science.

Dietz, D.N., 1965. Determination of average reservoir pressure from buildup surveys. J. Petrol. Technol. 17 (8), 955–959.

Hall, H.N., 1953. Compressibility of reservoir rocks. Trans. AIME 198, 309.

Haynes, B., Abdelmawla, A., Stromberg, S.G.L., 2008. Impact of pore volume compressibility on recovery from depletion drive & miscible gas injection in south Oman. In: SPE Paper 115274 Presented at the SPE Annual Technical Conference and Exhibition, Denver, Colorado, 21-24 September.

He, J., Ling, K., Pei, P., Ni, X., 2016. Calculation of rock compressibility by using the characteristics of downstream pressure change in permeability experiment. J. Petrol. Sci. Eng. 143, 121–127.

Hettema, M.H.H., Raaen, A.M., Naumann, M., 2013. Design and interpretation of laboratory experiments to determine the pore volume compressibility of sandstone. In: ARMA Paper 13-554 Presented at the 47th U.S. Rock Mechanics/Geomechanics Symposium, San Francisco, California, 23-26 June.

Hettema, M.H.H., Schutjens, P.M.T.M., Verboom, B.J.M., Gussinklo, H.J., 2000. Production-Induced compaction of sandstone reservoirs, the strong influence of field stress path. SPE Reservoir Eval. Eng. 3 (4), 342–347.

Iwere, F.O., Moreno, J.E., Apaydin, O.G., Ventura, R.L., Garcia, J.L., 2002. Vug characterization and pore volume compressibility for numerical simulation of vuggy and fractured carbonate reservoirs. In: SPE Paper 74341 Presented at the SPE International Petroleum Conference and Exhibition in Mexico, Villahermosa, Mexico, 10-12 February.

Jalalh, A.A., 2006a. Compressibility of porous rocks, part I. measurements of Hungarian Reservoir Rock Samples. Acta Geophys. 54 (3), 319–332.

Jalalh, A.A., 2006b. Compressibility of porous rocks, part II. New relationships. Acta Geophys. 54 (4), 399–412.

Khatchikian, A., 1996. Deriving Reservoir pore-volume compressibility from well logs. SPE Adv. Technol. 4 (1), 14–20.

Lachance, D.P., Andersen, M.A., 1983. Comparison of uniaxial strain and hydrostatic stress pore-volume compressibilities in the Nugget Sandstone. In: SPE Paper 11971 Presented at the SPE Annual Technical Conference and Exhibition, San Francisco, California, 5-8 October.

Lan, Y., Moghanloo, R.G., Davudov, D., 2017. Pore compressibility of shale formations. SPE J. 22 (6), 1–12.

Ling, K., He, J., Pei, P., Ni, X., 2014. A new method to determine pore compressibility. In: ARMA Paper 14-6964 Presented at the 48th U.S. Rock Mechanics/Geomechanics Symposium, Minneapolis, Minnesota, pp. 1–4 (June).

Mattar, L., McNeil, R., 1998. The flowing gas material balance. J. Can. Pet. Technol. 37 (2), 52–55.

Newman, G.H., 1973. Pore-volume compressibility of consolidated, Friable, and unconsolidated reservoir rocks under hydrostatic loading. J. Petrol. Sci. Eng. 25 (2), 129–134.

Narasingam, A., Siddhamshetty, P., Kwon, J., 2018. Handling spatial heterogeneity in reservoir parameters using proper orthogonal decomposition based Ensemble Kalman Filter for model-based feedback control of hydraulic fracturing. Ind. Eng. Chem. Res. 57 (11), 3977–3989.

Oliveira, G., Ceia, M., Missagia, R., Neto, I.L., Archilha, N., 2014. Pore volume compressibilities derived from Helium porosimetry and elastic measurements. In: SEG Paper 2014-1125 Presented at the 2014 SEG Annual Meeting, Denver, Colorado, USA, 26-31 October.

Oliveira, G.L.P.D., Ceia, M.A.R., Missagia, R.M., Archilha, N.L., Figueiredo, L., Santos, V.H., Neto, I.L., 2016. Pore volume compressibilites of sandstones and carbonates from Helium porosimetry measurements. J. Petrol. Sci. Eng. 137, 158–201.

Pauget, L., Specia, F., Boubazine, A., 2002. Reliability of laboratory porosity and pore compressibility obtained on unconsolidated deep-off shore and heavy-oil reservoirs. In: SPE Paper 77639 Present at the SPE Annual Technical Conference and Exhibition, San Antonio, Texas, 29 September-2 October.

Sampath, K., 1982. A new method to measure pore volume compressibility of sandstones. J. Petrol. Technol. 34 (6), 1360–1362.

Saxena, V., 2011. A novel technique for log-based pore volume compressibility in complex carbonates through effective aspect ratio. In: SPE Paper 149124 Presented at the SPE/DGS Saudi Arabia Section Technical Symposium and Exhibition, Al-khobar, Saudi Arabia, 15-18 May.

Seehong, O., Zheng, Z., Richin, C., 2001. Pressure-dependent pore volume compressibility – a cost effective log-based approach. In: SPE Paper 72116 Presented at the SPE Asia Pacific Improved Oil Recovery Conference, Kuala Lumpur, Malaysia, 6-9 October.

Siddhamshetty, P., Kwon, P., 2018. Model-based feedback control of oil production in oil-rim reservoirs under gas coning conditions. Comput. Chem. Eng. 112, 112–120.

Siddiqui, S., Funk, J.J., AI-Tahini, A.M., 2010. Use of X-ray CT to measure pore volume compressibility of Shaybah carbonates. SPE Reservoir Eval. Eng. 13 (1), 155–164.

Sun, H., 2015. Advanced Production Decline Analysis and Application. Elsevier, Amsterdam.

Tonnsen, R.R., Miskimins, J.L., 2011. Simulation of deep-coalbed-methane permeability and production assuming variable pore-volume compressibility. J. Can. Pet. Technol. 50 (5), 23–31.

Von Gonten, W.D., Choudhary, B.K., 1969. The effect of pressure and temperature on pore volume compressibility. In: SPE Paper 2526 Presented at the Fall Meeting of the Society of Petroleum Engineers of AIME, Denver, Colorado, 28 September-1 October.

Wolf, C., Russell, C., Luise, N., Chhajlani, R., 2005. Log-based pore volume compressibility prediction-A deepwater GoM Case Study. In: SPE Paper 95545 Presented at the SPE Annual Technical Conference and Exhibition, Dallas, Texas, pp. 9–12 (October).

Yi, X., Ong, S.H., Russell, J.E., 2005. Characterizing pore compressibility, reservoir compaction and stress path under uniaxial strain condition for nonlinear elastic rock. In: ARMA/USRMS Paper 05-791 Presented at Alaska Rocks 2005, the 40th U.S. Symposium on Rock Mechanics (USRMS), Anchorage, Alaska, pp. 25–29 (June).

Zaki, H., Wang, S.T., Salih, S., 1995. Pore-compressiblity study of Arabian Carbonate reservoir rocks. SPE Form. Eval. 10 (4), 207–214.

Zeng, Q., Wang, Z., 2017. A new cleat volume compressibility determination method and corresponding modification to coal permeability model. Transport Porous Media 119, 689–706.

Zimmerman, R.W., 1991. Compressibility of Sandstones. Elsevier, Amsterdam-Oxford-New York-Tokyo.